Jupiter's Magnetosphere and Aurorae Observed by the Juno Spacecraft During its First Polar Orbits

Authors: J. E.P. Connerney[1,2], A. Adriani[3], F. Allegrini[4], F. Bagenal[5], S. J. Bolton[4], B. Bonfond[6], S. W. H. Cowley[7], J.-C. Gerard[6], G. R. Gladstone[4], D. Grodent[6], G. Hospodarsky[8], J. Jorgensen[9], W. Kurth[8], S. M. Levin[10], B. Mauk[11], D. J. McComas[12], A. Mura[3], C. Paranicas[11], E. J. Smith[10], R. M. Thorne[13], P. Valek[4], J. Waite[4]

Affiliations:

[1]Space Research Corporation, Annapolis, MD, 21403, USA.

[2]NASA Goddard Space Flight Center, Greenbelt, MD, 20771, USA.

[3]Institute for Space Astrophysics and Planetology, National Institute for Astrophysics, Rome, 00133, Italy.

[4]Southwest Research Institute, San Antonio, TX, 78238, USA.

[5]Laboratory for Atmospheric and Space Physics, University of Colorado, Boulder, CO, 80303 USA.

[6]Institut d'Astrophysique et de Geophysique, Universite de Liege, Liege, B-4000 Belgium.

[7]University of Leicester, Leicester, LE1 7RH, United Kingdom.

[8]University of Iowa, Iowa City, IA, 52242, USA.

[9]National Space Institute, Technical University of Denmark, Kongens Lyngby, 2800, Denmark.

[10]Jet Propulsion Laboratory, Pasadena, CA, 91109, USA.

[11]Johns Hopkins University, Applied Physics Laboratory, Laurel, MD, 20723.

[12]Department of Astrophysical Sciences, Princeton University, Princeton, NJ, 08544, USA.

[13]Department of Atmospheric and Oceanic Sciences, University of California-Los Angeles, Los Angeles, CA, 90095, USA.

*Correspondence to: Jack.connerney@nasa.gov.

Abstract: The Juno spacecraft's unique polar orbit provided the first direct observations of the Jovian magnetosphere and auroral emissions from a vantage point above the poles. Juno's initial 53.5 day capture orbit spanned the Jovian magnetosphere from bow shock to the planet and back, providing magnetic field, charged particle, and wave phenomena context for the subsequent passage over the poles and first traverse of Jupiter's hazardous inner radiation belts. Juno's energetic particle and plasma detectors made the first measurements of electrons precipitating in the polar regions, exciting intense ultraviolet (UV) and infrared (IR) auroras, also observed simultaneously by Juno's UV and IR imaging spectrographs. Juno transited beneath the most intense parts of the radiation belts, passed a few thousand kilometers above the cloudtops at closest approach, well inside of the Jovian ring system, and recorded the electrical signatures of high velocity impacts with small particles as it traversed the Jovigraphic equator.

One Sentence Summary: Juno's instruments provide the first complete polar maps of Jovian UV aurorae, the first spatially resolved images of the IR southern aurorae, and the first in-situ direct measurements of precipitating charged particle populations exciting the aurora.

The Juno Mission serves two principal science objectives, the first of which is to understand the origin and evolution of Jupiter, as well as the formation of our solar system and planetary systems emergent about other stars. Servicing this objective, Juno's measurements probe deep inside Jupiter to constrain its interior structure and composition, using measurements of Jupiter's gravity and magnetic fields, atmospheric composition, and deep atmospheric circulation (*Bolton et al.,* this issue). The second science objective takes advantage of Juno's unprecedented close-in polar orbits to explore Jupiter's polar magnetosphere and intense aurorae [1]. From a vantage point above the poles, Juno's fields and particles instrumentation gather direct *in-situ* observations of the particle populations exciting the aurora, imaged simultaneously by Juno's ultraviolet (UV) and infrared (IR) imaging spectrographs.

Juno's instrument complement includes a comprehensive suite of fields and particle instruments for in-situ sampling of Jupiter's environment. Juno's magnetometer investigation (MAG) consists of a pair of vector fluxgate magnetometers and proximate star cameras for accurate mapping of the planetary magnetic field [2]. Juno carries an energetic particle detector (JEDI) measuring electrons in the energy range 30 – 800 keV and ions from 10 keV to > 1MeV [3] and a Jovian Auroral (plasma) Distributions Experiment (JADE) measuring electrons with energies of 0.1 to 100 keV and ions from 5 to 50 keV [4]. Jovian radio and plasma waves are recorded with instrumentation (Waves) spanning the spectrum from a few 10's of Hertz to >40 MHz [5]. Remote observations of the aurora are acquired by a long-slit ultraviolet spectrograph (UVS) counting individual UV photons [6] with wavelengths between 68–210 nm and a Jupiter infrared auroral mapping instrument (JIRAM) supporting imagery and spectrometry over a tailored range (2–5 μm) of infrared wavelengths [7].

Jupiter's dynamo generates the most intense planetary magnetic field in the solar system, with a dipole moment ~20,000 times that of Earth and surface (1 bar level) field magnitudes about 20 times greater than Earth's. The supersonic solar wind is slowed well upstream of Jupiter forming a bow shock (BS) where the ionized solar wind is abruptly decelerated and heated by the obstruction created by Jupiter's magnetic field. Downstream of the shock lies a region of turbulent flow called the magnetosheath, separated from the voluminous region within (the magnetosphere) by the magnetopause (MP). Throughout the magnetosphere, charged particle motion is guided by the magnetic fields originating within Jupiter's interior, and, to a lesser extent, currents distributed throughout the magnetosphere.

Juno encountered the Jovian bow shock just once (June 24, 2016, day of year 176) on initial approach to Jupiter, at a radial distance of 128 Jovian radii (1 R_j = 71,492 km). Multiple MP crossings were observed spanning the next 5 days (June 25-29, DOY 177-181) at radial distances of 74-114 Rj, prior to orbit insertion on July 4 (DOY 186). Juno's approach and first few orbits lie very nearly in the dawn meridian, so all BS and MP observations are representative of the dawn flank of Jupiter's magnetosphere. Observation of but one bow shock upon approach suggests that Juno encountered a bow shock that was expanding in size, a conclusion bolstered by the multiple BS encounters experienced (DOY 199-210) during the 53.5 day capture orbit at radial distances of 92 – 112 Rj before apojove on DOY 213 (~113 Rj), and at distances of 102 – 108 Rj after (DOY 221-224). Apojove during the 53.5 day orbits occurs at a radial distance of ~113 Rj, so Juno resides at distances of >92 Rj for little more than half of its orbital period (~29 days). Thus on this and the subsequent orbit, Juno encountered the MP boundary a great many times at radial distances of ~81 – 113 Rj.

Juno's traverse through the well-ordered portion of the Jovian magnetosphere is illustrated in Figure 1, in which the measured magnetic field magnitude is compared with a magnetospheric model derived from earlier flybys. The variation in magnetic field magnitude throughout most of the 10-day interval centered on closest approach to Jupiter (1.06 Rj) at 12:53 UT is well understood based upon prior knowledge of the planetary magnetic field [8] and that of the Jovian magnetodisc [9], a system of azimuthal currents flowing in a washer-shaped disc within a few Rj of the magnetic equator. Upon approach (DOY 235-237), precipitous decreases in the observed magnetic field magnitude are the result of Juno's traversal of the magnetic equator wherein magnetodisc currents effectively nullify the internal field. Outbound from perijove, Juno traveled at higher magnetic latitudes and did not penetrate the magnetodisc currents so close to Jupiter. Juno's first passage through the Jovian magnetosphere, both inbound and outbound, most closely resembled the inbound portion of the high-latitude Ulysses flyby [11]. All are well described by a magnetodisc model with substantially less current density per unit radius [12] compared to the that prevalent during the Voyager and Pioneer encounters.

The magnetic field observed in the previously unexplored region close to the planet ($r<1.3Rj$) was dramatically different from that predicted by existing spherical harmonic models, revealing a planetary magnetic field rich in spatial variation, possibly due to a relatively large dynamo radius [*Bolton et al.,* this issue]. But perhaps the most perplexing observation was one that was missing: the expected magnetic signature of field aligned currents (Birkeland currents) associated with the main aurora. A preliminary search failed to identify significant magnetic perturbations associated with Juno's traverse of field lines rooted in the main auroral oval.

Juno's Waves instrument made observations of radio and plasma wave phenomena throughout the first perijove as summarized in Figure 2. These are the first observations in the Jovian

magnetosphere obtained at low altitudes and crossing magnetic field lines mapped to Jupiter's complex auroras, and as such the first to invite comparison with terrestrial observations. Jupiter's auroral radio emissions are prominently displayed in Figure 2, panel (a), particularly after perijove. Many of the interesting features evident in the figure are organized by a fundamental mode of the plasma, the electron cyclotron frequency (simply related to magnetic field intensity by f_{ce}[Hz] = 28|B|[nT]). In particular, the radio emissions above this (white) line in Figure 2, panels (a) and (b), and even near the top of panel (c), are confined to frequencies at or above f_{ce}. These radio emissions are thought to be generated by the cyclotron maser instability (CMI) at frequencies at or just below f_{ce} [13]. Since these radio emissions closely approach the line at f_{ce} in several locations, and show intensification as they do so, it appears that Juno passed very close to (if not through) the source regions for these emissions for the first time.

Panels (c) and (d) of Figure 2 show the electric and magnetic components, respectively, of waves at frequencies below 20 kHz. The two intensifications of this emission just after 12:00 and near 13:30 UT demarcate Juno's passage over Jupiter's main auroral oval. These features are thought to be whistler-mode hiss, often called auroral hiss [14, 15] and correspond to features in the energetic electron distributions described below. These waves exist at frequencies below the lower of f_{ce} and f_{pe}, the electron plasma frequency, related to the electron density n_e by $n_e = (f_{pe}/8980)^2$ with n_e expressed in cm^{-3} and f_{pe} in Hz. Surprisingly, the lack of features in the wave spectrum identifying the electron plasma frequency leads to the conclusion that the plasma density over the northern polar cap is very low, perhaps less than 10^{-3} cm^{-3}. This leads to the identification of the emissions in panels c and d prior to 12:00 and those above 20 kHz but below f_{ce} in panel b as ordinary mode radio emission called continuum radiation. The intensifications

in panels c and d with a period of 15 minutes after 14:00 are suggestive of a link to pulsating auroras reported by Earth-based observers in both ultraviolet and x-ray wavelengths.

The intense burst of noise centered near perijove in panel (c) and extending into panel (b) is associated with dust grains impacting the Waves electric antenna (or perhaps the spacecraft). The grains impact the spacecraft with a relative velocity of > 60 km/s, with sufficient kinetic energy to vaporize the grain and a portion of target material, from which a fully-ionized high-temperature gas ($\sim 10^5$ K) evolves. The expanding plasma cloud from each impact produces an impulse in the electric channel of the Waves receiver that can be counted, yielding an estimated impact rate of a few per second near the jovigraphic equator. These grains are presumably being lost from Jupiter's ring system into the planetary atmosphere.

Emissions observed centered around perijove in panel (b) between about 20 and 80 kHz are likely ordinary mode radio emissions that can propagate below f_{ce} and above f_{pe}. The source for these emissions is unknown and it is not known whether these emissions are related to the trapped continuum radiation.

Electron and ion observations obtained throughout this 24-hour interval are presented in Figure 3. The broad bright region between about 0400 and 0800 represents a period of time when the spacecraft dipped into Jupiter's radiation belts where high electron and ion intensities are encountered [16]. This period is centered on a local minimum in (dipole) magnetic latitude, at radial distances between 7 and 10 Rj, and ~4 Rj above the magnetic equator. This is close to, but not within, the current-carrying region (+/- 3 Rj) prevailing in magnetodisc models fitted to prior observations confined to lower latitudes. These observations, and the suppressed intensities encountered near hours 20-22, at radial distances between 9 and 11 Rj, also at a local minimum in magnetic latitude (but now ~5 Rj below the magnetic equator), suggest a somewhat broader

distribution of magnetodisc currents about the magnetic equator relative to more distant crossings.

As the spacecraft traveled out of that region, at about 0835, Juno's JEDI and JADE sensors observed localized electron intensification with JEDI electron distributions (panel b) symmetrically aligned with the local magnetic field direction, with the largest intensifications near 0° and 180° pitch angles [17]. This is the rather subtle feature seen in all panels of Figure 3 just after the broad intensification between 400 and 0800 UT. This occurred when Juno, at a distance of about 6 RJ from Jupiter, crossed the magnetic field lines that map to the main northern auroral oval. The relatively dark region between ~8:40 and ~12:00 represents the traversal of the polar cap, the region poleward of the northern main auroral oval. That same dark region is repeated for the southern polar pass, between ~1400 and ~1800. Within both of these polar cap regions, JEDI observed mono-directional, upward-directed electron beams confined narrowly to the measured magnetic field directions. Those beams are evidenced in panel (b) of Figure 3 with the brightening that occurs near 0° pitch angle between 0840 and 1200, and then near 180° between 1400 and 1800. Beyond ~1830 the spacecraft skims a region with magnetic field lines that map to the main auroral oval, and electron particle structures are observed with low contrast bi-directional electron beaming. Note that the all of electron beams observed by JEDI (> 30 keV) and discussed herein are angular beams; the energy distributions are monotonic and do not have peaks in the energy distributions that are common in Earth auroral distributions. Near the center of Figure 3, between ~1200 and ~1330, ion and electron sensors responded to additional auroral structures and also intense radiation within the high-latitude horns of the radiation belts, examined in more detail (greater temporal and spatial resolution) in Figure 4. In

this brief span of time, Juno traversed field lines mapped to the northern auroral oval, the inner radiation belt, and the southern auroral oval.

Figure 4(b) shows more clearly, on the extreme left, the bi-directional, but asymmetric electron beams observed by the JEDI electron detectors within the northern polar cap. The bi-directionality is important because it is the downward-traveling electron beam (near 180° on the left, across the northern polar cap, and near 0° on the right, across the southern polar cap) that deposits energy into Jupiter's upper atmosphere, potentially powering Jovian auroral emissions. Figure 4(c) provides an estimate of the energy deposition contributed by 30 – 1000 keV electrons, calculated using electron intensities within 15° of the downward field line (the region spanning the radiation belts, where very high energy electrons penetrate detector shielding, has been excluded).

Energy depositions up to ~80 mW/m^2 are observed in the northern hemisphere and up to ~200 mW/m^2 in the southern hemisphere, both observed within the geometric loss cones. These energy depositions are sufficient by themselves to account for typical auroral UV luminosities at Jupiter [18], although we expect that electrons with energies < 30 keV may contribute substantially to the total energy deposition pending further analyses of JEDI and JADE observations. This observation implies that Juno passed beneath the acceleration region powering Jovian auroral emissions, at least on this occasion.

Surprisingly, the highest JEDI energy deposition in the southern hemisphere (between 1330 and 1340 UT) was associated with a non-beaming diffuse precipitation, as demonstrated by the character of the pitch angle distribution at that time. While mechanisms for the generation of angular beams with monotonic energy distributions have been discussed in the context of Earth's

polar regions [19, 20], the context there may be different, in that intense aurora are not generally associated with those beams.

At the very center of Figure 4 (~1245) there appears a localized population of particles (ions or electrons; the species is not known) centered at what we suppose to be the time of the actual magnetic equator crossing, in agreement with that computed using spherical harmonic models of the magnetic field (~20° latitude at ~92° sys III longitude). The feature is localized in pitch angle because the loss cones are huge in this region. This feature is puzzling and analysis is ongoing.

During the period near closest approach, the JADE ion sensor observed three distinct ion populations (Figure 5). Starting in the northern hemisphere at ~12:13 UT, JADE-I observed three ion populations, each separated in energy per charge (E/Q) and having a mean energy of ~5, 0.2, and 0.02 keV/Q, respectively. The mean energy of the two higher energy ion populations decreased with time until their abrupt disappearance at ~12:20 UT, coinciding with the spacecraft moving equatorward of the Io flux tube footprint [21]. The TOF spectra (not shown) show strong peaks for mass per charge (m/q) of 1 (H^+), 8 (O^{++}), 10.67 (S^{+++}), 16 (O^+ or S^{++}), and a weaker peak for 32 (S^+). The strongest signal is from m/q of 16. These ions have energies > 0.1 keV/Q, appear to be moving together, and are evidently Iogenic in origin [22]. A third, lower energy population of 10's of eV protons is also observed during this timeframe. These low energy protons may be outflowing from Jupiter. During this pass JADE did not detect a significant population of H_3^+ ions. These three distinct ion distributions reappeared in the southern hemisphere starting at ~13:21 as Juno moved to poleward of the Io flux tube footprint. The energies and trends seen in these ion distributions are similar to that observed in the northern hemisphere.

The electron distributions showed similar energy dependence as the ions. Starting at 12:10 UT, JADE-E began to observe ~1 – 10 keV electrons whose energy decreased to below the 0.1 keV lower limit of the sensor by 12:16 UT as the spacecraft moved towards Jupiter's equator. A similar profile was observed in the southern hemisphere between 13:25 and 13:35 UT. These electrons are of lower energy than those responsible for the UV emissions of Jupiter's main auroral oval and likely reflect the electron distributions in Jupiter's plasma disk.

Juno's UV and IR imaging spectrographs captured images and spectra of the Jovian northern and southern aurora from a unique vantage point above the poles. The northern auroral oval is offset from the rotation pole by virtue of the geometry of Jupiter's non-dipolar magnetic field, and most longitudes can be imaged from near-equatorial latitudes. Thus many images of the northern aurora have been obtained over the years in the IR [23] and UV [24,25] using earth-based and earth-orbiting assets (e.g., Hubble Space Telescope). The southern aurora is more closely confined to high polar latitudes and has not been well mapped until now.

Figure 6 displays the first complete polar maps of Jupiter's northern and southern UV polar aurorae and the first detailed polar map of Jupiter's southern aurora in the IR. This montage is organized with orthographic projections of emission intensity in the leftmost column, with spectral color ratios in the rightmost column. The UV maps are an assemblage of slit scans across the polar region acquired with every rotation of Juno (30.725s). The UVS field of view is steered by the rotation of the spacecraft and the orientation of the UVS scan mirror at the instrument entrance aperture. The UV brightness map is a measure of the energy flux of the precipitating electrons that generate the auroral emissions, while the color ratio, measuring the amount of methane absorption at wavelengths <140 nm, is a proxy for the precipitating electron energy. The more energetic the precipitating electron, the deeper it will penetrate into the

atmosphere before it impacts an atmospheric molecule (H_2); UV photons emerging from deep in the atmosphere are more likely to be absorbed, resulting in a larger color ratio. Color ratios have long been observed from Earth orbit [26, 27], but are necessarily obtained at much larger slant paths compared to the overhead views afforded by Juno.

These first close-up glimpses of Jupiter's night-side UV aurora show a very intense and strongly absorbed (i.e., having high color ratio) patch of outer emissions (located at system III longitudes ~230°-280°) in the northern polar region and a complex structure protruding from the main auroral emission into the polar region in the south (located at system III longitudes ~20°-40°). Aside from these noteworthy morphological features, substantial brightness and color ratio differences are seen between the hemispheres, but it is not clear yet if they should be attributed to hemispheric asymmetries [26] or to temporal variations.

The IR intensity image of the southern aurora, in the leftmost column of Figure 5, is the first of its kind, assembled from 25 L-band filter images (3.3-3.6 micron). Intensity observed in this band is dominated by the presence of multiple H3+ emission lines, observed with high signal-to-noise against a background effectively darkened by absorption due to methane [28]. This image was obtained within a span of 12 minutes at about 6 hours after perijove. The spatial resolution of a single pixel is ~150 km. The thickness of the main oval is quite variable along the arc. Like the UV aurora, the IR aurora is thicker on the dusk side of the planet (to the right in Figure 5) and thinner on the dawn side. Note, however, that the UVS image in Figure 5c was acquired ~5 hrs prior to the IR image, and therefore nearly opposite in local time from the JIRAM image in 5e.

The UV and IR auroral images both clearly show Iogenic emissions [29, 30], either at the instantaneous IFT footprint or along the very long wake left behind the Io footprint, and emissions associated with the other Galilean satellites [31]. The Europa wake is also noticeable with more difficulty in the IR image as it partially mixed with the main oval structure. The JIRAM instrument has a limited capability of independent pointing and it can only observe in the plane orthogonal to the spacecraft spin axis. The IR color ratio map (Figure 5 panel f) provides an indication of the temperature of the polar atmosphere at the altitude of the H_3^+ emission. Figure 5f accounts for all the spectral observation taken over the Southern Polar aurora during a period of several hours almost covering the diurnal hours of the Jovian day. Then is not possible to identify a specific direction of the Sun like in the JIRAM imager picture (Figure 6e). The map in Figure 6f is compiled from JIRAM spectral observations by taking the ratio of two prominent H_3^+ emission lines (3.57 μm and the 3.67 μm). This ratio is dependent upon temperature, ranging from ~1.34 at 1100 K to ~1.7 at 700 K [32]. Preliminary analysis of JIRAM spectra suggests that the polar cap region interior to the main oval and between the longitude interval 30°-90° W is generally colder than the main oval.

The typical three Jovian auroral regions (the outer emissions, the main emissions and the inner emissions) can be easily identified in both the UV [25] and IR [33], together with well-identified sub-structures, such as the Io and Ganymede footprints [34], the large regions of UV emission associated with plasma injection signatures [35, 36] and the main emission discontinuity around noon. The overall aurora brightness level is somewhat dim, but not atypically so [37], and the UV color ratio values are also in the same range as previously observed [26,27]. While there is much similarity between the UV and IR auroras, there are notable differences related to the emission mechanisms at work in both cases. UV emissions are more directly responsive to

precipitating particles and as such evidence rapid time variations [37]. In contrast, IR emissions are thermally exited and provide a measurement of upper atmospheric temperature and thereby a measure of energy deposition, whether by particle precipitation or joule heating. Thus the IR aurora varies more slowly in response to energy input [28, 38] and provides a valuable diagnostic of the transfer of angular momentum from Jupiter to (ionized) mass flowing outward in its magnetosphere [39].

Juno has provided the first observations of fields and particles in the polar magnetosphere of Jupiter as well as exquisite high-resolution images of the auroras at UV and IR wavelengths. Juno's first periapsis pass has opened the door to a new understanding of Jupiter's space environment and rotation-dominated magnetospheres in general. While many of the observations have terrestrial analogs it appears that different processes are at work in exciting the aurora and in communicating the ionosphere-magnetosphere interaction. We observed plasmas upwelling from the ionosphere, providing a mechanism whereby Jupiter helps populate its magnetosphere. The surprising weakness of the magnetic field-aligned electric currents associated with the main aurora, and the broadly distributed nature of electron beaming in the polar caps, suggest a radically different conceptual model of Jupiter's interaction with its space environment. The (precipitating) energetic particles that appear in association with Jovian auroral emissions are very different from the peaked energy distributions that power the strongest auroral emissions at Earth. Juno, in passing either through or very close to source regions of the auroral radio emissions, has gathered rich detail beyond the scope of this early report. In the next few years, Juno will add numerous additional periapsis passes to complete Juno's exploration of Jupiter's polar magnetosphere.

References and Notes:

[1] Bagenal, F., Adriani, A., Allegrini, F., et al. (2013) Magnetospheric science objectives of the Juno mission", *Space Sci. Rev.,* 1-69. doi:10.1007/s11214-014-0036-8.

[2] Connerney, J. E. P., Benn, M., Bjarno, et al. (2017) The Juno Magnetic Field Investigation, *Space Sci. Rev.,* doi: 10.1007/s11214-017-0334-z.

[3] Mauk, B.H., Haggerty, D.K., Jaskulek, S.E. et al. (2014) The Jupiter Energetic Particle Detector Instrument (JEDI) Investigation for the Juno Mission, *Space Sci. Rev.,* doi:10.1007/s11214-013-0025-3.

[4] McComas, D.J., Alexander, N., Allegrini, F. et al. (2013) The Jovian Auroral Distributions Experiment (JADE) on the Juno Mission to Jupiter, *Space Sci Rev*. dos:10.1007/s11214-013-9990-9.

[5] Waves utilizes two sensors: an electric dipole antenna mounted on the aft flight deck oriented with its sensitive axis parallel to Juno's y axis and a search coil magnetometer mounted to the spacecraft with its sensitive axis parallel to Juno's z axis (the rotational axis). Search coil output is processed (by the Low Frequency Receiver) over a frequency range of 50 Hz to 20 kHz. Electric field signals are processed via an identical channel. Waveforms from these channels are Fourier transformed to produce a logarithmically-spaced spectrum with ~16 channels/decade. A mid-frequency band included in the Low Frequency Receiver processes electric dipole signals from 10 kHz to 150 kHz. These waveforms are Fourier transformed to produce a logarithmically-spaced spectrum with ~15 channels/decade. Redundant High Frequency Receivers process electric dipole signals between 100 kHz and 40 MHz. This receiver includes channels from 3 to 40 MHz (1 MHz bandwidth) in which amplitudes are detected in a sweep frequency receiver mode. Between 100 kHz and 3 MHz, waveforms are acquired and processed to generate a logarithmically-spaced spectrum with ~18 channels/decade. All of these spectral components can be collected every 1, 10, or 30 seconds depending on telemetry allocation. Waveforms from each of these receivers may be collected in burst modes for limited intervals of time at low duty cycle. A 1-MHz band tuned to include the local electron cyclotron frequency is also used for burst waveforms from the High Frequency Receiver.

[6] Gladstone, G. R., Persyn, S. C., Eterno, J. S., et al. (2014) The Ultraviolet Spectrograph on NASA's Juno Mission, *Space Sci. Rev.*, doi:10.1007/s11214-014-0040-z.

[7] Adriani A., Filacchione, G., Di Iorio, T. D. , et al. (2014) JIRAM, the Jovian Infrared Auroral Mapper. *Space Sci. Rev.,* DOI 10.1007/s11214-014-0094-y.

[8] Connerney, J.E.P. (2015) Planetary magnetism. Volume 10: Planets and Satellites. In G. Schubert and T. Spohn, (Eds.) *Treatise in Geophysics*, Elsevier, Oxford, UK, vol. 10.06, 195-237. ISBN: 978-0-444-63803-1.

[9] Connerney, J.E.P., Açuna, M.H. & Ness, N.F. (1981) Modeling the Jovian current sheet and inner magnetosphere. *J. Geophys. Res., 86,* 8370 - 8384.

[10] Connerney, J. E. P., M. H. Acuña, N. F. Ness, and T. Satoh (1998) New models of Jupiter's magnetic field constrained by the Io flux tube footprint, *J. Geophys. Res.,* 103(A6), 11,929–11,939.

[11] Balogh, A., Dougherty, M. K., Forsyth, R. J., et al., (1992) Magnetic field observations during the Ulysses flyby of Jupiter, *Science* 257, 1515-1518.

[12] The Pioneer 10, Voyager 1, Voyager 2, and outbound leg of the Ulysses flyby were well modeled within 30 Rj of Jupiter using the magnetodisc model cited in reference 9 with a current disc in the magnetic equator having an inner and outer radius of 5 and 50 Rj, respectively; a thickness of +/- 2.5 or 3 Rj, and a current constant of 225. The Ulysses inbound trajectory and Juno's first perijove both required substantially less current (~45% less) and a larger outer radius of the current-carrying magnetodisc (90 Rj).

[13] Treumann, R. A. (2006), The electron-cyclotron maser for astrophysical application, *Astron. Astrophys. Rev.*, 13(4), 229–315, doi:10.1007/s00159-006-0001-y.

[14] Gurnett, D. A., (1966) A Satellite Study of VLF Hiss, *J. Geophys. Res.*, 71, 5599-5615.

[15] Whistler mode identification of these emissions is tentative. There is some evidence for very low plasma densities in this region of the magnetosphere, with associated plasma frequencies possibly in the range of a few hundred Hz. If so, the spectrum may instead be dominated by the z-mode since whistler modes cannot exist above the plasma frequency.

[16] de Soria-Santacruz, M., Garrett, H. B., Evans, et al., (2016) An empirical model of the high-energy electron environment at Jupiter, J. Geophys. Res. Space Physics, 121, doi:10.1002/2016JA023059.

[17] Charged particles travel in helical trajectories about the magnetic field. The angle between a particle's velocity vector and the magnetic field direction is referred to as the "pitch angle", which, in a non-uniform magnetic field, varies with the ratio between the perpendicular and parallel components of the particle's velocity. This important quantity determines whether a particle will bounce back and forth, trapped in a non-uniform magnetic field, or for sufficiently small pitch angles, travel far enough to be absorbed in the atmosphere.

[18] Clarke, J. T. (2012) Auroral Processes on Jupiter and Saturn. In A. Keiling, E. Donovan, F. Bagenal and T. Karlsson (eds.), *Auroral Phenomenology and Magnetospheric Processes: Earth And Other Planets*, American Geophysical Union, Washington, D. C. doi: 10.1029/2011GM001199.

[19] Carlson, C. W. et al., (1998) FAST observations in the downward auroral current region: Energetic upgoing electron beams, parallel potential drops, and ion heating, *Geophys. Res. Lett,* 25, 2017, doi:10.1029/98GL00851.

[20] Mauk, B. H., and J. Saur (2007) Equatorial electron beams and auroral structuring at Jupiter, *J. Geophys. Res.,* 112, A10221, doi:10.1029/2007JA012370.

[21] The Io Flux Tube (IFT) footprint is the area in ionosphere that maps along magnetic field lines to the satellite Io, orbiting in the Jovigraphic equator at ~5.9 Rj radial distance. It is sometimes referred to the "instantaneous" IFT footprint, to distinguish it from the oval traced out in the polar region by the locus of IFT footprints generated as Io moves about Jupiter in system III longitude. The "extended" IFT footprint, or "tail", is the trailing portion of the (instantaneous) footprint.

[22] Kupo, I., Mekler, Y. and Eviatar, A. (1976) Detection of Ionized Sulphur in the Jovian Magnetosphere, *Astrophys. J.* 205, L51-L53. See review by Thomas, N., F. Bagenal, T. W. Hill, and J. K. Wilson (2004) The Io neutral clouds and plasma torus, in *Jupiter, The Planet, Satellite*

and Magnetosphere, eds. F. Bagenal, T. Dowling, and W. McKinnon, vol. 561, Cambrige Univ. Press, Cambridge, U. K.

[23] Stallard, T., Miller, S., Melin, H. (2012) Clues on Ionospheric Electrodynamics from IR Aurora at Jupiter and Saturn. In Auroral Phenomenology and Magnetospheric Processes: Earth and Other Planets. Geophys. Mono. Series, vol. 197, pp. 215–224.

[24] Clarke, J.T., Grodent, D., Cowley, S., et al., (2005) Jupiter's aurorae. In F. Bagenal, T.E. Dowling, and W.B. McKinnon (Eds.), *Jupiter: The planet, satellites, and magnetosphere*, Cambridge University Press, Cambridge, UK.

[25] Grodent, D. (2015) A Brief Review of Ultraviolet Auroral Emissions on Giant Planets *Space Sci Rev* 187: 23. doi:10.1007/s11214-014-0052-8

[26] Gérard J.-C., Grodent, D., Radioti, A., Bonfond, B., Clarke, J. T. (2013) Hubble observations of Jupiter's north–south conjugate ultraviolet aurora. *Icarus* 226, 1559–1567, doi:10.1016/j.icarus.2013.08.017

[27] Gustin, J., Grodent, D., Ray, L. C., et al., (2016) Characteristics of north jovian aurora from STIS FUV spectral images, Icarus, 268, 215-241, ISSN 0019-1035, http://dx.doi.org/10.1016/j.icarus.2015.12.048.

[28] Connerney, J.E.P., & Satoh, T. (2000) The H_3+ ion: A remote diagnostic of the Jovian magnetosphere. *Phil. Trans. R. Soc. Lond. A, 358,* 2471 - 2483.

[29] Connerney, J.E.P., Baron, R., Satoh, T., & Owen, T. (1993) Images of excited H_3+ at the Foot of the Io Flux Tube in Jupiter's atmosphere. *Science, 262,* 1035 - 1038.

[30] Clarke, J.T., Ballester, G.E., Trauger, J., et al., (1996) Far-Ultraviolet imaging of Jupiter's aurora and the Io "footprint" with the Hubble Space Telescope Wide Field Planetary Camera 2. *Science, 274,* 404 - 409.

[31] Clarke, J.T., Ajello, J., Ballester, G.E., et al., (2002) Ultraviolet emissions from the magnetic footprints of Io, Ganymede, and Europa on Jupiter. *Nature, 415,* 997 - 1000.

[32] Dinelli, B. M., LeSuer, C. R., Tennyson, J., Amos, R. D., (1995) Ab initio ro-vibrational levels of H_3^+ beyond the Born-Oppenheimer approximation, *Chem. Phys. Lett.*, 232, No. 3, 295-300.

[33] Satoh, T., & Connerney, J.E.P. (1999) Jupiter's H_3+ emissions viewed in corrected Jovimagnetic coordinates. *Icarus, 141,* 236 - 252.

[34] Bonfond, B. (2012) When moons create aurora: The satellite foot-prints on giant planets, in Auroral Phenomenology and Magnetospheric Processes: Earth And Other Planets, edited by A. Keiling et al., pp. 133–140, AGU, Washington, D.C., doi:10.1029/ 2011GM001169.

[35] Mauk, B. H., J. T. Clarke, D. Grodent, J. H. Waite, C. P. Paranicas, and D. J. Williams (2002) Transient aurora on Jupiter from injections of magnetospheric electrons, Nature, 415, 1003–1005.

[36] Bonfond, B., Grodent, B., Gérard, J.-C., et al., (2012) Auroral evidence of Io's control over the magnetosphere of Jupiter, Geophys. Res. Lett., 39, L01105, doi:10.1029/2011GL050253.

[37] Clarke, J. T., et al. (2009) Response of Jupiter's and Saturn's auroral activity to the solar wind, J. Geophys. Res., 114, A05210, doi:10.1029/ 2008JA013694.

[38] Baron, R., Owen, T., Connerney, J.E.P., Satoh, T., & Harrington, J. (1996) Solar wind control of Jupiter's H_3+ aurorae. *Icarus, 120,* 437 - 442.

[39] Hill, T.W., 1979 Inertial limit on corotation. *J. Geophys. Res.* 84, 6554–6558.

Acknowledgements:

We thank the many Project and support staff at the Jet Propulsion Laboratory, Lockheed Martin, and the Southwest Research Institute, for their contributions to the successful design, implementation, and operation of the Juno spacecraft. We also thank the scientists, engineers, technicians, and operations support staff at each of the institutions that provided Juno's science payload: Goddard Space Flight Center, the Applied Physics Laboratory, the University of Iowa, and the Technical University of Denmark, in addition to the institutions listed above. We also thank the Italian Space Agency (ASI), B.M Dinelli and F. Fabiano for support of the JIRAM contribution to the Juno mission. The Belgian contribution to the UVS investigation is made possible via support from BELSPO. The Jet Propulsion Laboratory manages the Juno mission for the principal investigator, Scott Bolton, of Southwest Research Institute in San Antonio. The Juno mission is funded by NASA and is part of the New Frontiers Program managed at NASA's Marshall Space Flight Center in Huntsville, Ala.

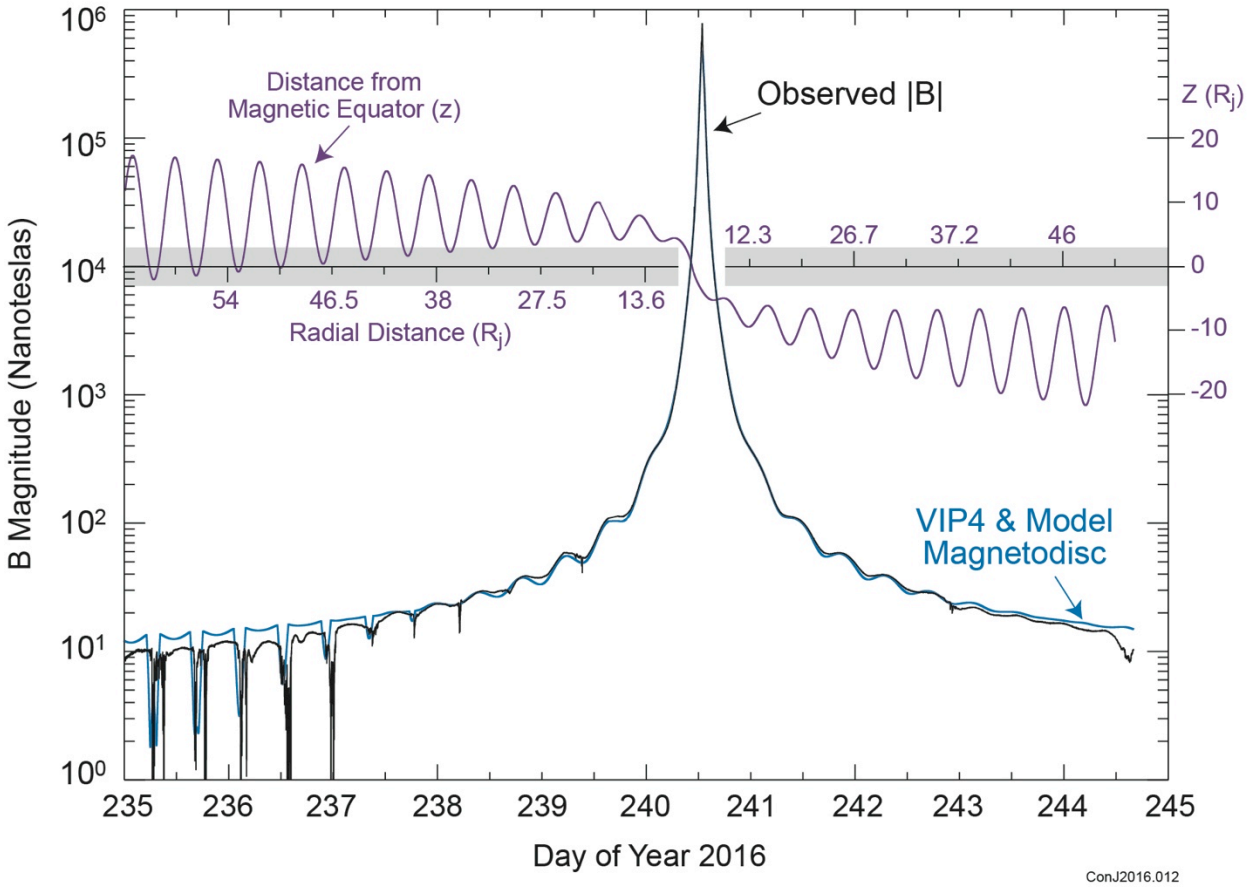

Fig. 1.: Measured magnetic field magnitude (black, solid) and distance from the magnetic equator (purple) as a function of time and distance from Jupiter during Juno's first perijove pass, compared to a model (blue) that combines the planetary magnetic field (VIP4 spherical harmonic [10] model) with that of the magnetodisc, a system of azimuthal currents confined to within ~3 Rj of the magnetic equator (shaded region). The magnetic field magnitude increases by over six orders of magnitude on approach to perijove, where a field of 7.776 G was observed.

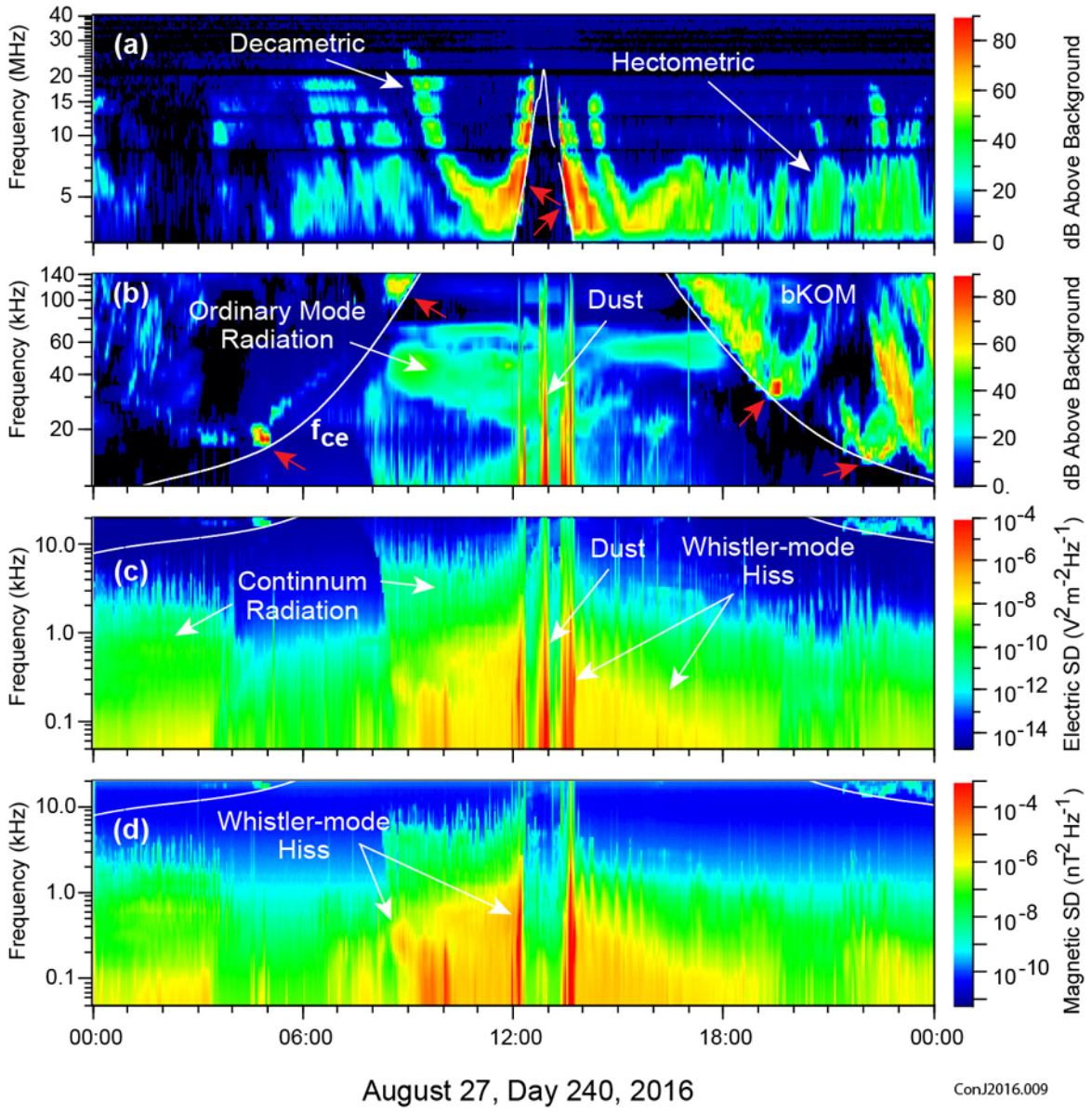

Fig. 2.: Radio and plasma wave observations in Jupiter's polar magnetosphere during Juno's first perijove pass. The intensity of one electric component (panels a-c) of waves as a function of frequency (50 Hz to 40 MHz) and time and one magnetic component (panel d) as a function of frequency (50 Hz to 20 kHz) and time is indicated by the color bar. The white curve in all panels peaking in frequency near perijove is the electron cyclotron frequency calculated from the magnitude of the measured magnetic field by $f_{ce}[Hz] = 28|B|[nT]$. Red arrows in panels a and b identify emissions observed with increasing intensity just above f_{ce} that may indicate proximity to or passage through emission source regions.

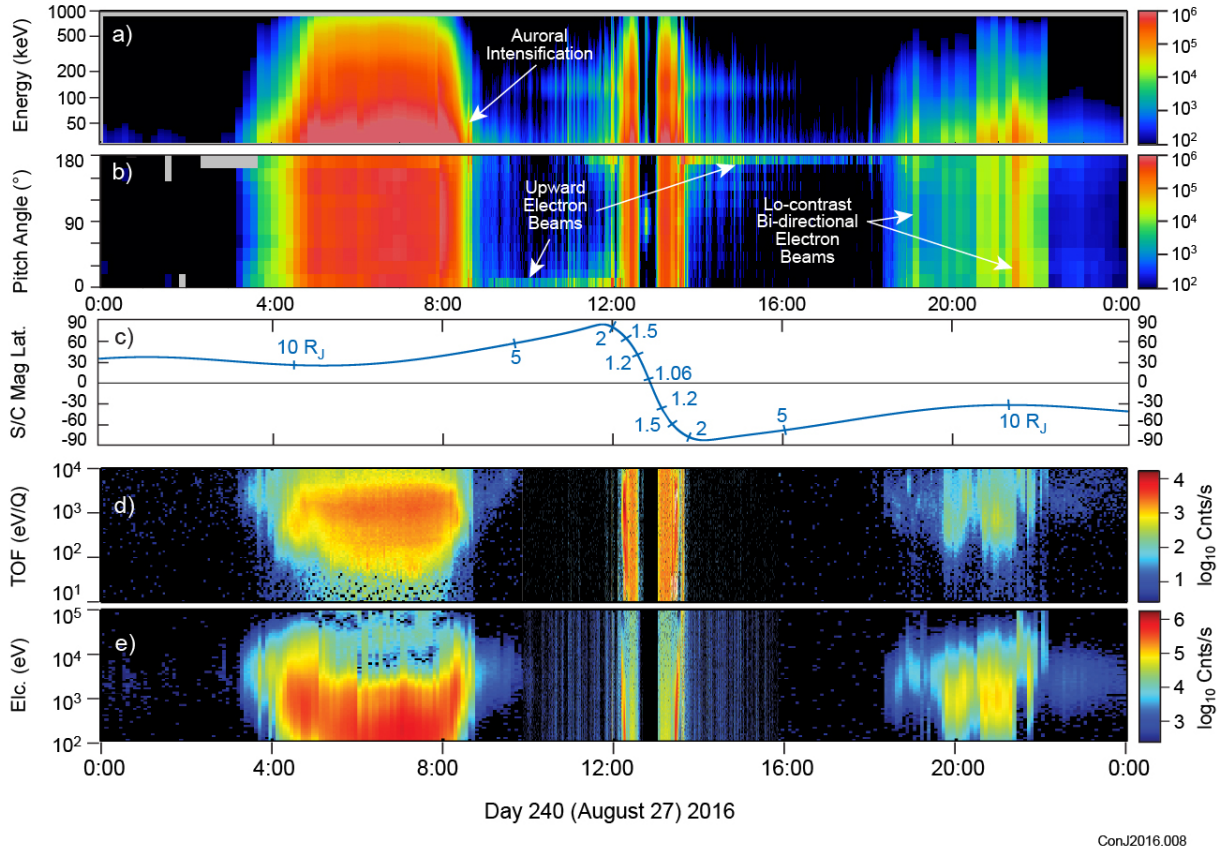

Fig. 3. A 24 hour display, centered on the Juno perijove pass, of energetic electron data from the JEDI instrument in panels (a) and (b) and the lower energy JADE plasma data for ions (panel d) and electrons (panel e). The electron energy spectrogram in panels (a) and (e), with energy expressed in kilo-electron-volts, or keV, sums all angular look directions, whereas the dynamic electron pitch angle spectrogram in panel (b) sums all instrument energy channels. The Juno spacecraft's (dipole) magnetic latitude and radial distance from Jupiter as a function of time is shown in panel (c). Note that in panel (a), from ~9:00 to 16:00 UT, the horizontal band centered on ~150 keV is an artifact caused by intense foreground electrons (energies > 700-800 keV) that fully penetrate JEDI's electron sensor leaving behind a fraction of their actual energy. The JADE ion spectrogram (panel d) sums ion counts over all directions and ion species (units of keV/charge, i.e., keV/Q).

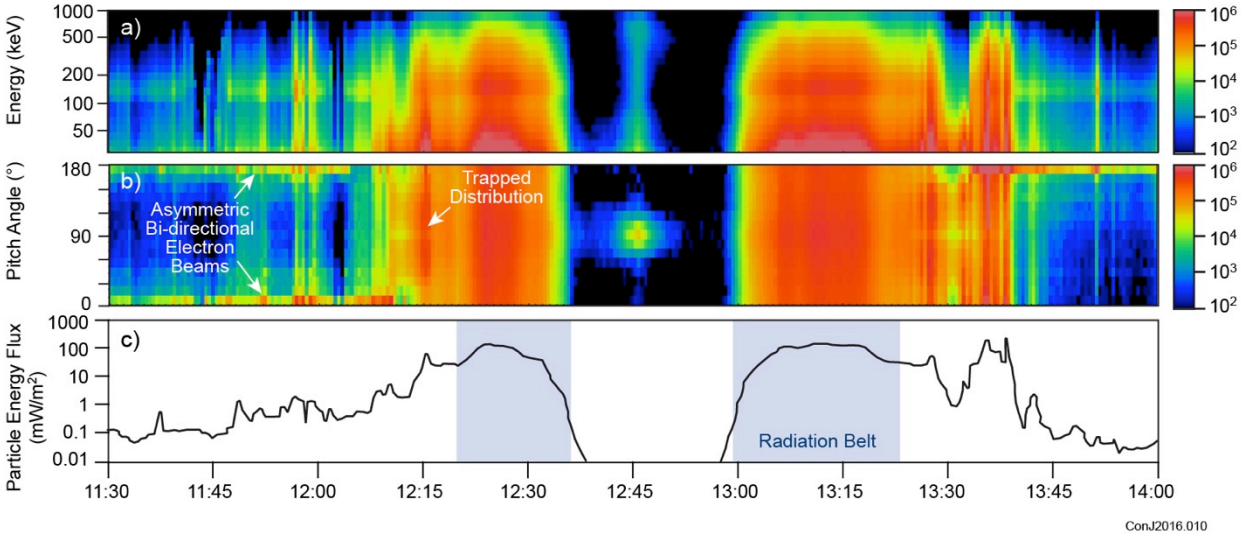

Fig. 4. JEDI electron energy and pitch angles (panels a and b as in Figure 3) observed during Juno's polar passages, showing (extreme left) field-aligned, bi-directional, but asymmetric electron beams. Downward traveling beams (near 180°, left and near 0°, right) can deposit energy into Jupiter's atmosphere, exciting auroral emissions. Notably, upward traveling electron beams are in evidence throughout both polar caps. Panel (c) shows an estimate of the energy deposition from 30 – 1000 keV downward-traveling electrons, using intensities summed over an angle within 15° of the downward field line direction (excluding the radiation belts, where very high energy electrons penetrate detector shielding).

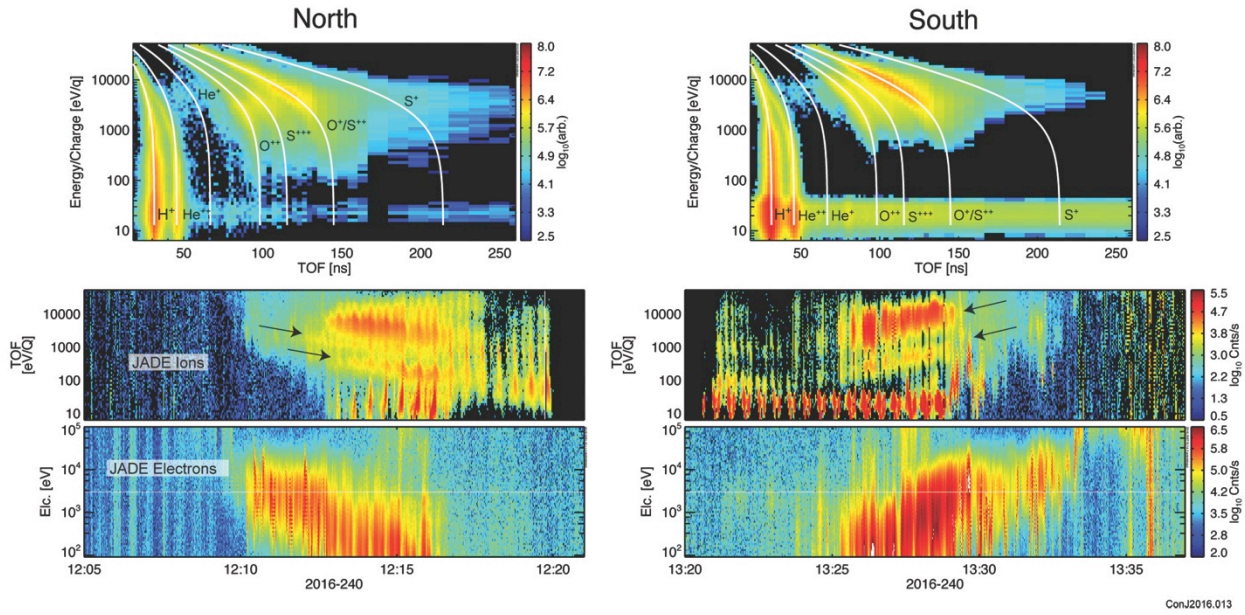

Figure 5: Observations of the plasma at latitudes equatorward of the main auroral oval in the northern (left) and southern (right) hemispheres. The top panels show the Energy / Time of Flight (TOF) distributions from the time ranges of the lower plots. Overlaid on the Energy/TOF plots are traces showing the position of mass / charge (m/q) of 1 (H^+), 2 (H^+ or He^{++}), 4 (He^+), 8 (O^{++}), 10.7 (S^{+++}), 16(O^+ or S^{++}), and 32 (S^+). Due to interactions in the carbon foil of the TOF section, the peak at m/q of 2 is primarily due to incident protons. The total ions as a function of energy and time are plotted in the middle panels, and the electrons observed by JADE-E a in the bottom panel.

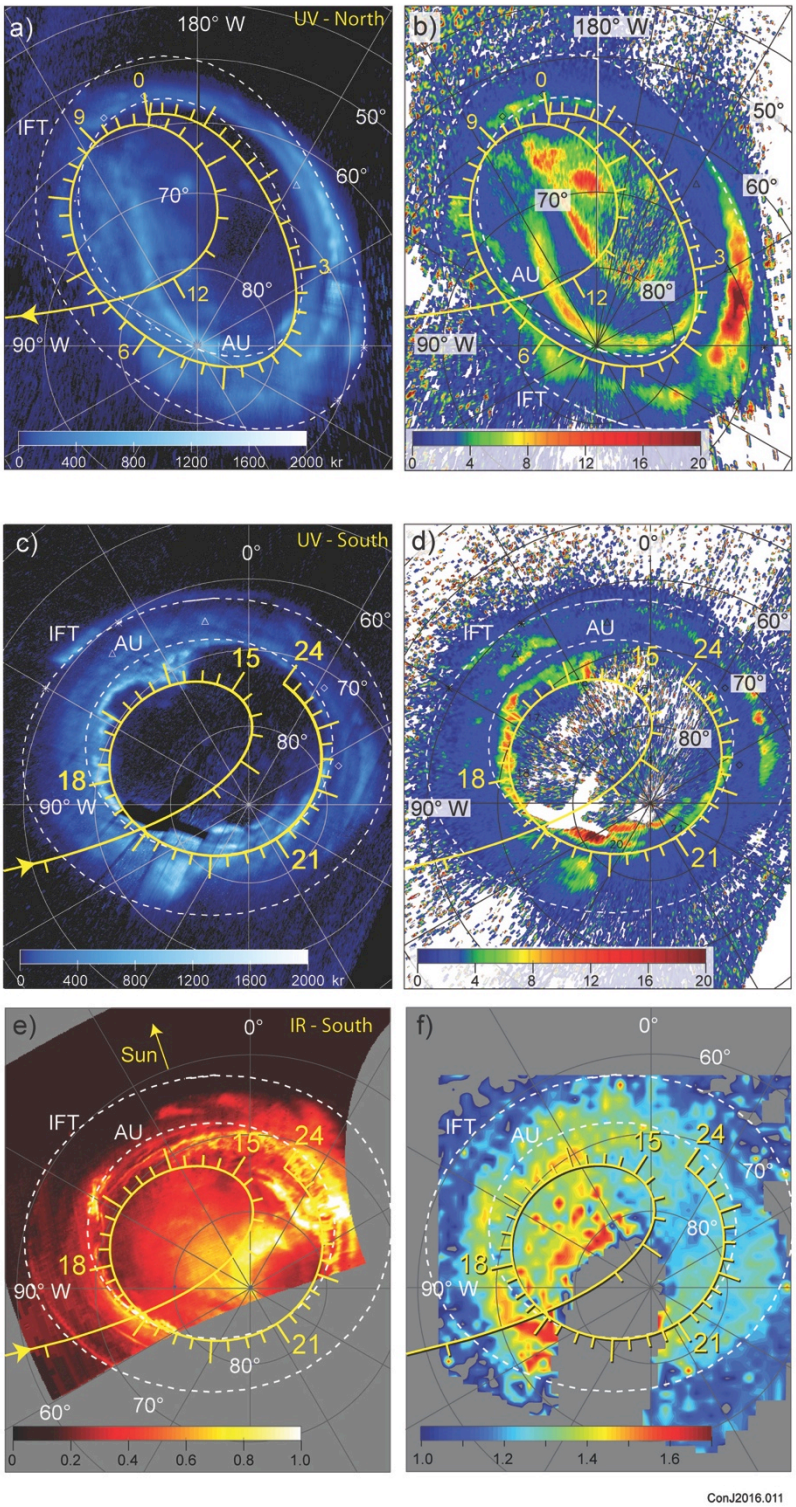

Fig. 6. Orthographic polar projections at the 1 bar level of the ultraviolet (panels a-d) and infrared (e-f) auroral emissions, comparing auroral intensities (left column) and spectral color ratios (right column) with the model auroral oval (innermost dashed oval) and Io footprint (outer dashed circle) computed using the VIP4 model internal field and a model magnetodisc. The

footprint of the spacecraft is shown by the solid line, with hourly tic marks to facilitate comparison with *in-situ* fields and particles observations shown in Figures 1-4. Top panels are northern UV aurora, center and bottom panels compare UV and IR southern aurora, respectively. UV intensities are summed between 60-180 nm and UV color ratios are given as 155-162nm/123-130nm. UVS north (south) polar data acquired between 09:52:35 and 10:40:59 (13:22:39 and 14:34:12) UT on DOY 240, 2016. The infrared aurora (left) is a mosaic of 25 L band filter images (3.3-3.6 um) obtained with 1 s integration time from between 18:09:21 and 18:22:10 UT on DOY 240, showing emission due to the H_3^+ ion. The spectral color ratio (right) is obtained from JIRAM spectra acquired between 14:45 and 19:51 UT as the ratio of two H_3^+ emission lines (3.57 μm /3.67 μm) that is diagnostic of temperature (blue relatively cold, red, hot). Gray regions are areas devoid of data.